

Effect of nitrogen doping method on the activity of Fe-N-C catalysts based on carbon xerogels for fuel cells

L. Álvarez-Manuel^{1*}, C. Alegre¹, P. Napal¹, D. Sebastián¹, M.J. Lázaro¹

¹Instituto de Carboquímica, CSIC. C/. Miguel LuesmaCastán, 4. 50018 Zaragoza

(*) lalvarez@icb.csic.es

The development of active and inexpensive non-precious metal catalysts is a necessary and essential requirement to replace currently used Pt-based catalysts, in order to reduce the cost of polymer electrolyte fuel cells (PEFC). [1] Catalysts based on the Fe-N-C structure develop high electroactivity towards the oxygen reduction reaction (ORR), the limiting reaction in fuel cells. To increase the catalysts activity, Fe must be dispersed in a carbon material with a high surface area. In this context, carbon xerogels are excellent candidates, as their main properties can be easily tailored: porosity, electrical conductivity and surface chemistry. [2] The meso/macroporosity of carbon xerogels can be designed by modifying the conditions of the synthesis process, while microporosity can be generated by subsequent carbonization/activation treatments [3]. In the present work, on the basis of carbon xerogels with an optimal ratio of micro/meso/macroporosity, we investigate the effect of two different methods of nitrogen-doping in the catalytic activity of Fe-N-C catalysts. Catalysts are evaluated both in half-cell and single-cell configurations and their activity is correlated to their physical-chemical features.

Organic xerogels (OXG) were synthesized by a sol-gel synthesis method from resorcinol and formaldehyde. The first doping method consisted of mixing the OXG with urea followed by pyrolysis at 800°C (N-CXG-1). The second doping method, consisted of a first pyrolysis of OXG into carbon xerogel (CXG) at 800°C, and then mixing CXG with urea followed by a second thermal treatment at 800°C (N-CXG-2). All thermal treatments were carried out in inert atmosphere for 1h duration. The Fe doping was made by mixing either the N-CXG-1 or the N-CXG-2 in a planetary ball mill with iron acetate. The obtained powder was pyrolyzed in N₂ atmosphere at 1050 °C for 1h, obtaining Fe-N-CXG-1 and Fe-N-CXG-2. [5] Subsequently, these materials were treated by a series of acid treatments in HClO₄ in order to eliminate inactive iron particles, followed by a thermal treatment at 950 °C in N₂ flow. The textural features of the carbon xerogels were determined by means of N₂ and CO₂ physisorption. The physical-chemical characteristics of the catalysts were determined by X-ray photoelectron spectroscopy (XPS), optical emission spectroscopy with inductive coupled plasma (ICP-OES), and elemental analysis (EA). The activity of the catalysts towards the ORR was determined in a three electrode cell with a rotating disk electrode (RDE) and O₂-saturated 0.5 M H₂SO₄ electrolyte. Membrane-electrode assemblies (MEAs) were prepared by hot-pressing of cathode (Fe-N-C catalyst, 4 mg cm⁻²) and anode (commercial Pt/C, 0.2 mg_{Pt} cm⁻²) with Nafion®212R membrane. The electrodes were prepared by spraying the catalyst on GDL-39BC (Sigracet) gas diffusion layer. A Fuel Cell Technologies Inc. test station was used to evaluate the MEA performance at a cell temperature of 80°C and 100%RH.

Table 1 shows the N/C atomic ratio determined by EA and XPS. Figure 1 presents the high-resolution N1s spectra with the N speciation. The Fe-N-CXG-2 catalyst presents a higher N/C and a higher contribution of N-Fe bond compared to Fe-N-CXG-1.

	EA	XPS
	N/C	N/C
N-CXG-1	0.07	0.12
N-CXG-2	0.07	0.09
Fe-N-CXG-1	0.02	0.03
Fe-N-CXG-2	0.05	0.06

Table 1. N/C atomic ratios calculated by EA and XPS.

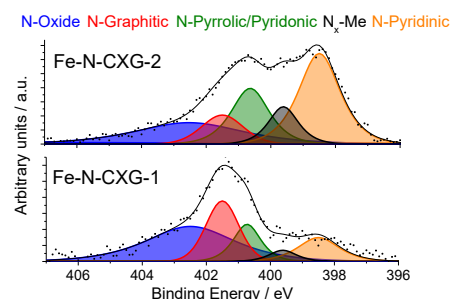


Figure 1. High-resolution N1s spectra fitted with individual peaks.

Figure 2 (a) shows the catalysts activity towards the ORR measured in a three-electrode cell system. Fe-N-CXG-2 presents a significantly higher activity compared to Fe-N-CXG-1, what correlates with its higher N/C and N-Fe content. The half-wave potential for Fe-N-CXG-2 is 110 mV lower than the one for the commercial benchmark catalyst, Pt/C (40wt% Pt, Johnson Matthey). RDE measurements at different rotation speeds (400 to 2500 rpm) were adjusted to the Koutecky-Levich (KL) equation in order to determine the number of electrons transferred during the ORR (Figure 2 (b)). As expected, the ORR on Pt/C goes through 4e⁻. Both Fe-N-C catalysts present similar slopes than Pt/C, meaning that ORR in these catalysts also goes through a four-electron pathway [6].

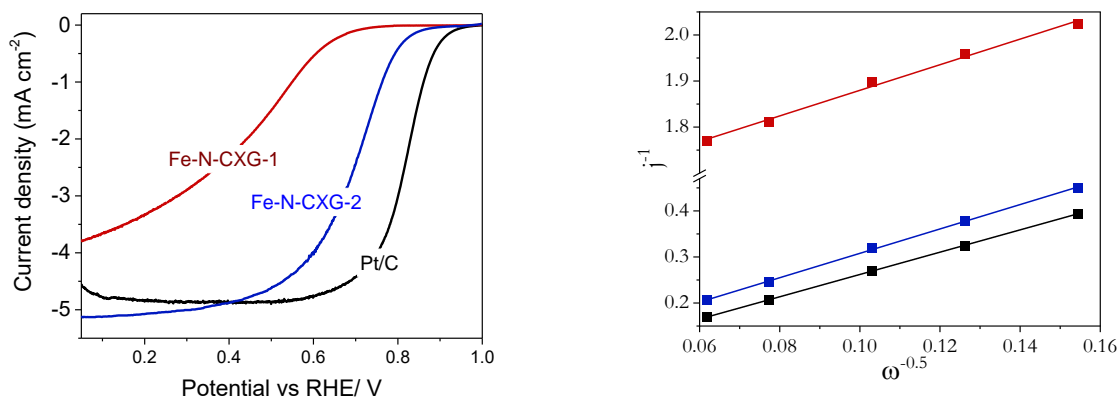


Figure 2. (a) Polarization curves for the ORR, in RDE at 1600 rpm in O_2 -saturated 0.5M H_2SO_4 . (b) Koutecky-Levich plot j^{-1} vs. $\omega^{-0.5}$ at 0.6V vs. RHE.

The Fe-N-C catalysts activity and durability was also studied in a PEFC single cell. Fig. 3 (a) shows the polarization curves at the beginning (0h) and after 20h operation at 0.5 V while Fig. 3 (b) shows the power density curves. The Fe-N-CXG-2 catalyst exhibits a polarization curve about 100 mV better than Fe-N-CXG-1, in line with 3-electrode cell results. Therefore, the maximum power density is about 80% higher for Fe-N-CXG-2. After 20h operation, the Fe-N-CXG-2 also shows a lower loss in performance compared to its counterpart Fe-N-CXG-1. From these results, the two step nitrogen-doping method appears more effective for the preparation of Fe-N-C catalysts based on carbon xerogel substrate since a larger amount of Fe-N species is favoured according to XPS results.

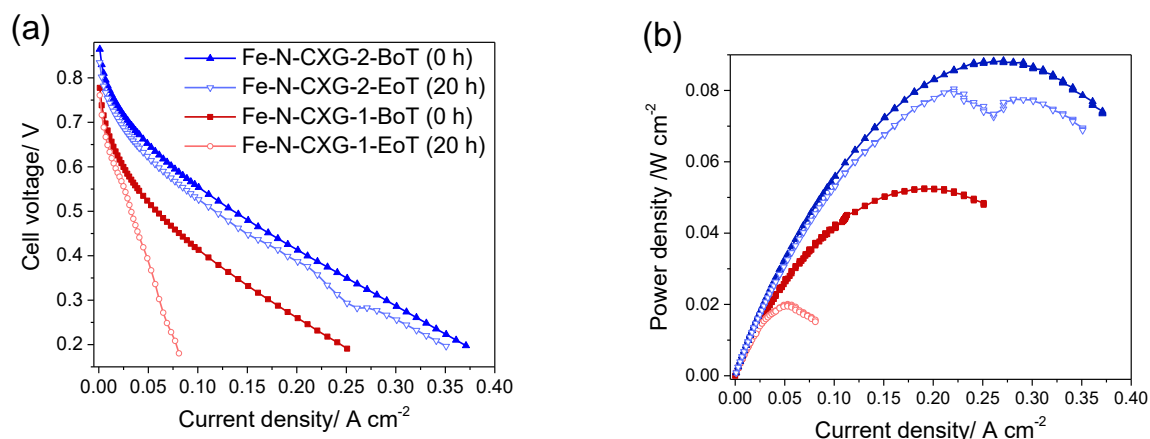


Figure 3. (a) Polarization curves for MEAs comprising a cathode made with Fe-N-CXG after and before of 20 h operation test. (b) Power density curves. Cell temperature 80°C, 100% RH, hydrogen/oxygen (150/130 kPa-g backpressure).

Acknowledgements

The authors wish to thank the Ministry of Science and Innovation and the AEI(MCIN/AEI/10.13039/501100011033) for the funding received with the reference project PID2020-115848RB-C21 and the Government of Aragon for funding the T06-20R group. L. Álvarez-Manuel wish to thank the Government of Aragon for her pre-doctoral contract.

References

- [1] Z. Chen, D. Higgins, A. Yu, L. Zhang, J. Zhang, *Energy Environ. Sci.* **4** (2011) 3167–3192.
- [2] M. Canal-Rodríguez, N. Rey-Raap, J. A. Menéndez, M. A. Montes-Morán, J. L. Figueiredo, M. F. R. Pereira, A. Arenillas, *Microporous/Mesoporous Mat.* **293** (2020) 1387-1811.
- [3] H. Jin, H. Zhang, H. Zhong, J. Zhang, *Energy Environ. Sci.* **4** (2011) 3389–3394.
- [4] R. Gokhale, S. Thapa, K. Artyushkova, R. Giri, P. Atanassov, *ACS Appl. Energy Mater.* **1**(2018), 3802–3806.
- [5] E. Proietti, F. Jaouen, M. Lefèvre, N. Larouche, J. Tian, J. Herranz, J. Dodelet, *Nat. Commun.* **2** (2011) 416-427.
- [6] B. P. Vinayan, T. Diemant, R. J. Behn, S. Ramaprabhu, *RSC Adv.* **5** (2015) 66494–66501